JOURNAL OF MATERIALS SCIENCE **38** (2003) 3713–3720

Dielectric permittivity and loss of hydroxyapatite screen-printed thick films

C. C. SILVA, A. F. L. ALMEIDA
Departamento de Quimica Orgânica e Inorgânica-UFC, Caixa Postal 6030, CEP 60455-760, Fortaleza, Ceará, Brasil

R. S. DE OLIVEIRA
Departamento de Física-Universidade Estadual do Ceará-UECE,

A. G. PINHEIRO, J. C. GÓES, A. S. B. SOMBRA
Laboratório de Telecomunicações e Ciencia e Engenharia dos Materiais (LOCEM), Departamento de Física, Universidade Federal do Ceará, Campus do Pici, Caixa Postal 6030, 60455-760 Fortaleza, Ceará, Brasil
E-mail: sombra@ufc.br

In this paper we did a study on the structural and electrical properties of bioceramic hydroxiapatite (HA) thick films. The films were prepared in two layers using the screen printing technique on Al_2O_3 substrates. Mechanical alloying has been used successfully to produce nanocrystalline powders of hydroxyapatite (HA) to be used in the films. We also look for the effect of the grain size of the HA in the final properties of the film. The samples were studied using X-ray diffraction, scanning electron microscopy (SEM), energy-dispersive spectroscopy (EDS) and electric measurements. We did a study of the dielectric permittivity and the loss of the films in the radio-frequency of the spectra. The X-ray diffraction (XRD) patterns of the films indicates that all the peaks associated to HA phase is present in the films. One can notice that, for all the films there is a decrease of the DC with the increase of the frequency. The values of the dielectric constant of the films are in between 4 and 9 (at 1 KHz), as a function of the flux material concentration. The loss is decreasing as we increase the frequency for all the films. These results strongly suggests that the screen-printing HA thick films are good candidates for applications in biocompatible coatings of implant materials but also for the insulating materials of electronic circuits and dielectric layer in bio-sensors. © *2003 Kluwer Academic Publishers*

1. Introduction

Hydroxyapatite (HA, $Ca_{10}(PO_4)_6(OH)_2$) is widely used in reconstructive orthopaedic and dental surgery, both as massive filling [1] of bone gaps and as a surface coating. In the latter case it promotes adhesion between prostheses and bone [2]. This material is present in substantial amounts in the mineralised tissue of the vertebrates-60–70% of the mineral phase of the human bone [3]. In order to propose the biosynthetic process of the bone, the synthesis of HA was developed in this work. The human bone is formed basically by an organic phase and other mineral phases. In the organic phase, the fibers of collagen serve as a matrix for the precipitation of HA, determining the structure of the crystals. The collagen gives the bone its elastic resistance. The mineral phase is formed by HA.

Several processes [4, 5] are used to produce HA of wide application as a temporary substitute for the human bone [5–9]. Hydrothermal synthesis is characterised by the reaction of aqueous solutions in closed recipients under controlled temperature and/or pressure. The temperature can be elevated above the boiling point of the water, reaching the pressure of vapour saturation. One specific method of hydrothermal synthesis consists of submitting an aqueous solution containing Ca^{2+} and PO_4^{3-} to high temperatures (200°C–500°C). Thus a calcium phosphate compound is obtained which is able to maintain the morphological structure of the original material. The hydrothermal method has been widely used [9] for the preparation of materials for prosthetic purposes. These materials are attractive for various applications include coatings of orthopedic and dental implants, alveolar ridge augmentation, maxillofacial surgery, otolaryngology, and scaffolds for bone growth and as powders in total hip and knee surgery.

The HA ceramic, however, are much more brittle than living bone and ordinary bioceramics, such as tricalcium phosphate (TCP), alumina ceramics (α-Al_2O_3) etc. Under this view, much effort has been devoted in recent years to the development of processing methods to deposit HA on corrosion resistant alloys. Recent advancements in synthesis of HA coatings include

eletrophoretic deposition [10, 11], electrochemical deposition [12], laser pulse deposition [13], ion beam deposition [14] and more recently sol-gel deposition [15, 16]. The sol-gel approach received more attention than others over the past 10 years because of it's low temperature nature and ease of processing and forming. Others deposition methods include for the HA thin film have been reported which include sputtering [17]. Recently, the pulsed laser deposition (PLD) methods has been applied to produce pure crystalline HA thin films [18, 19].

In this work we report the application of mechanical alloying technique to produce HA, from elementary powders. The advantage of this procedure remains on the fact that melting is not necessary, the powders are nanocrystalline and exhibits extraordinary mechanical properties [20–22].

It can also be easily shaped (injected, compacted, etc.) into any geometry. The production, and the study of the properties of HA ceramics is important in view of possible applications of HA in the area of orthopedics and dentistry emerges as one of the most important applications of this material.

Mechanical alloying is a powerful technique to obtain any quantity of powder with controlled microstructure [22]. Nowadays the technique is used in a large range of commercial products, moreover, most of these applications are on metallic domain. The mechanical alloying technique was already used, by our group, to obtain nanocrystalline ferroelectric ceramics of lithium niobate LN ($LiNbO_3$) [20]. Lithium Niobate-LN is a ferroelectric material with a trigonal crystal structure, with melting point at 1253°C and Curie temperature at 1210°C. It is characterised by large pyroelectric, piezoelectric, electro-optic, photo-elastic coefficients and is naturally birefringent. Furthermore the technique is very effective to produce nanocrystalline piezoelectric ceramics.

In this paper, we describe the preparation of HA thick films, prepared from a nanocrystalline HA ceramic obtained by mechanical alloying. The HA thick film was prepared over a thick film of silver. The structural properties of the films is discussed with emphasis on the electrical properties. These properties are important in view of possible applications of these films in the fabrication of biological sensors.

2. Experimental procedure

2.1. HA nanocrystalline powder

In this paper mechanical alloying has been used successfully to produce nanocrystalline powders of hydroxyapatite (HA) using the procedure [22]:

$$10Ca(OH)_2 + 3P_2O_5 \xrightarrow{\text{IMPACTS}} Ca_{10}(PO_4)_6(OH)_2 + 9H_2O \quad \text{(Reaction 3)}$$

Commercial oxides $Ca(OH)_2$ (Vetec, 97% with 3% of $CaCO_3$), P_2O_5 (Vetec, 99%), were used in the HA preparation [22]. For this reaction the material was ground on a Fritsch Pulverisette 5 planetary mill with the exact proportionality between the oxides given in above equation. Milling was performed in sealed stainless steel vials and balls under air, with 370 rpm as rotation speed. The powder mass to the ball mass ratio used in all the experiments was near 1/9. To avoid excessive heat the milling was performed in 60 min milling steps with 30 min pauses. Mechanical alloying was performed for 60 h of milling to produce the ceramic HA3.

2.2. Paste preparation

The paste was prepared from the suspension of organic material (resin, organic solvent and some additive to improve rheological behavior of the paste) and powders (HA), in relation 30:70. The organic part used in the film preparation was chitosan. Chitosan is a polymer, which contains β-1-4 linked 2-amino-2-deoxy-D-glucopyranose repeat units and is readily obtained by the N-deacetylation of chitin, a naturally abundant polysaccharide. This biopolymer, is the structural component of the cuticles of crustaceans, insects, and mollusks and is also found in the cell of some microorganisms. A number of biomedical applications have also been envisaged. Chitosan and its derivatives have explored as membranes for dialysis, wound healing accelerators and carriers for controlled drug delivery [23]. To have a better adhesion between paste and substrate (Al_2O_3) it was added a low temperature melting glass in powder form. The used glass is a commercial product (Glasstécnica), is basically a borosilicate structure. The concentration of the glass in the total mass of the samples is indicated by the reference Y in the indication of the samples (see Table I). The samples are indicated by HA3GY, where $Y = 5$, 10, 15, 20 and 25% is the indication of the glass presence (mass%) in the total mass of the powder, used in the film preparation.

2.3. Substrates and electrodes

Alumina substrates (Al_2O_3) were used as a commercial product (Engecer). The electrode material were

TABLE I Dielectric Permittivity measurements (K), thickness (e), dielectric loss (D), and the crystallite size obtained from the X-ray diffraction (Fig. 2) of the thick films samples. Mass relation Ca/P obtained from energy dispersive spectroscopy (expected value for HA is 2.15) for the HA3 ceramic and thick films HA3G5, HA3G10 and HA3G15. For all the samples $L = 1$ cm

Samples	Thickness (μm)	K [$\varepsilon'_{33}/\varepsilon_0$] (1 KHz)	D ($\varepsilon''_{33}/\varepsilon'_{33}$) (1 KHz)	Crystallite size (nm)	Ca/P mass ratio	ρ g/cm^3
HA3(powder)				38.9	2.10	
HA3G5	351	4,96	0,27	46	1.62	1.06
HA3G10	328	5,75	0,10	44	2.37	
HA3G15	305	5,38	0,58	47,5	2.37	
HA3G20	328	8,73	0,48	46,3		
HA3G25	325	8,22	0,72	42,5		1.51

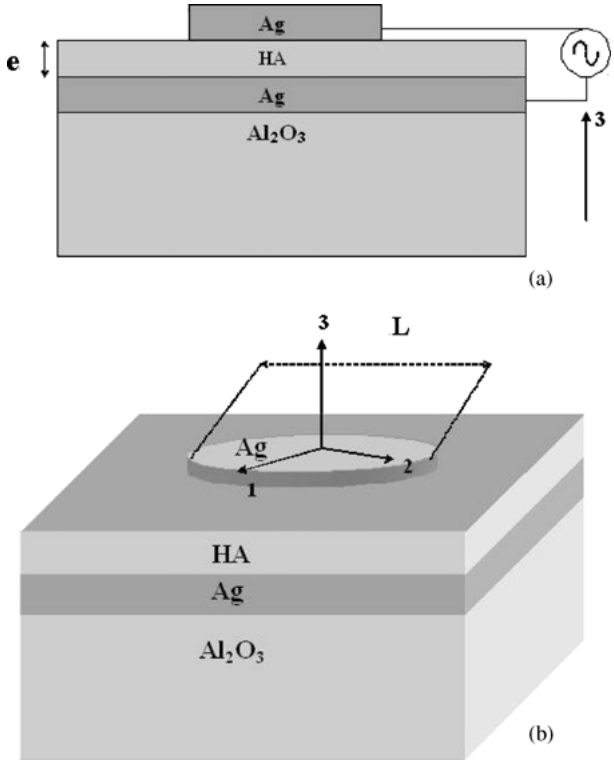

Figure 1 A rectangular coordinate assigned to the sample for the measurement of piezoelectric and dielectric constant in the thick film structure.

produced for the screen printing technique (Joint Metal-PC200) in the geometry described in Fig. 1.

2.4. Preparation of the films

The bottom electrodes (Ag) were screen printed on the Al_2O_3 substrate and fired at 850°C for 1 h. On the fired electrode, a HA layer was screen printed and sintered at for 1 h. After firing the dielectric layer, the upper electrode (Ag) was deposited, and after that dried and fired at the same temperature-time regime as for the bottom electrode. The obtained films usually had thickness that ranged from 20 to 400 μm, depending on the number of layers. All the films used in these measurements were composed of two layers. For the films in the series HA3G(Y) (see Table I), the film was subjected to the firing process: 100°C for 1 h + 400°C for 1 h + 700°C for 1 h (first layer). 100°C for 1 h + 400°C for 1 h + 700°C for 1 h (second layer).

It was observed that the increase of the glass content lead to an increase of the density (ρ) of the thick film (see Table I).

2.5. X-ray diffraction

The X-ray diffraction (XRD) patterns were obtained at room temperature (300 K) by step scanning using powdered samples. We used five seconds for each step of counting time, with a Cu K_α tube at 40 kV and 25 mA using the geometry of Bragg-Brentano. The analysis of the crystallite size (L_c) of the HA phase has been done for all samples using the Scherrer's equation,

$$L_c = \frac{k\lambda}{\beta \cos\theta}$$

where k is the shape coefficient (value between 0.9 and 1.0), λ is the wave length, β is the full width at half maximum (FWHM) of each phase and θ is the diffraction angle. For this purpose, we chose the single peak near 25.8 degree within the pattern and according to $P6_3/m$ space group of HA. We have used the LaB_6 (SRM 660-National Institute of Standard Technology) powder standard pattern to determine the instrumental width ($w_{inst} = 0.087°$) and afterward to calculate the crystallite size via Equation 1. The β parameter has to be correct using the following equation:

$$\beta = \sqrt{w_{exp}^2 - w_{inst}^2}$$

where w_{exp} correspond to experimental FWHM obtained for each sample. The crystallite size for the milled ceramic and for the film was obtained, assuming coefficient $k = 1$.

2.6. Scanning electron microscopy

The photomicrograph of the films of HA, were obtained on a Scanning Electron Microscope, Phillips XL-30, operating with bunches of primary electrons ranging from 12 to 20 keV, in rectangular lyophilized samples, covered with a layer of carbon of 30 nm of thickness.

2.7. Dielectric measurements

The dielectric measurements were obtained from a HP 4291A Material Impedance Analyzer in conjunction with a HP 4194 Impedance Analyzer, which jointly cover the region of 100 Hz to 1.8 GHz. In Fig. 1 one has the sample geometry we used for the dielectric measurements. Rectangular coordinates are assigned to the samples as shown in Fig. 1. The 1-2 plane is the sample plane, and the 3 axis is perpendicular to the plane of the sample. The electrodes are circular (Ag) prepared using the screen printing technique. Our study is trying to understand the dielectric properties of the HA thick films. We prepared different samples with different glass concentration on the HA films. The glass concentration was changed from 5% to 25% in the film preparation (see Table I). For the HA ceramic one prepare a nanocrystalline powder prepared by mechanical alloying. We did a study of the dielectric permittivity (K) and loss (D), of the films. The role played by firing process of the film and the role played by the amount of glass in the structural properties of the film is also discussed.

3. Results and discussion

3.1. X-ray diffraction

Fig. 2 shows the X-ray diffraction (XRD) patterns of the films together with the XRD of the powder (HA3)

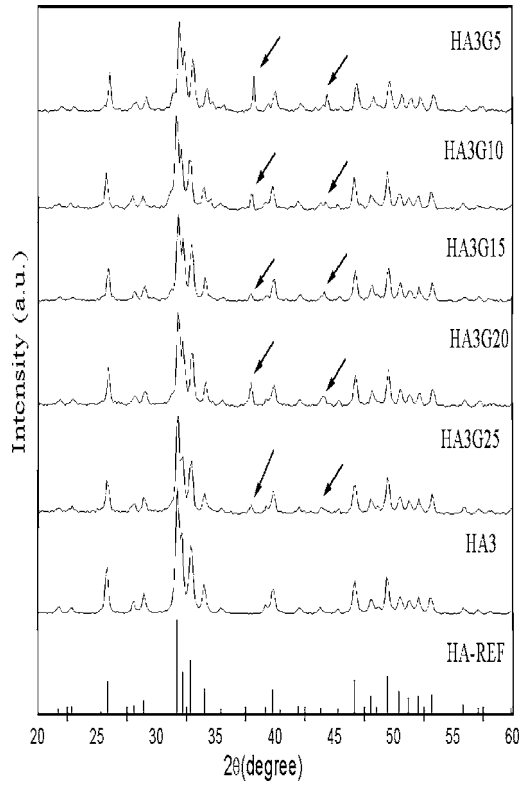

Figure 2 XRD patterns of the ceramic HA3 and thick films HA3G5, HA3G10, HA3G15, HA3G20 and HA3G25 and literature data for HA.

used in the film preparation (see Table I). The XRD of the powder HA3 shows that all the peaks associated to HA is present (see Table I). For this ceramic the crystallite size is estimated in 38.9 nm (see Table I). In the same figure one starts with the XRD of sample HA3G5. For this sample one can easily notice all the peaks associated to HA. However the crystallite size associated to HA is around 46 nm (see Table I). One can associate the increase of the crystallite size to the firing process that the film was submitted. One can also notice the presence of two little peaks (indicated by arrows in the figure), that are probably associated to the presence of the flux material (powder glass) that was used to improve the adhesion between the paste and the substrate. These peaks are probably associated to the presence of the glass in the film structure. The glass which is a commercial product (basically a borosilicate structure) is probably producing a new crystalline phase through the reaction with HA or alone, in view of the high temperatures that were used in the film preparation (see page 6 in the preparation of the film section). These temperatures should be enough to crystallize the flux material. If one starts increasing the presence of the glass (G = 10, 15, 20 and 25%) these peaks are still present (see Fig. 2). One can also conclude the HA crystallite size is in average around 46 nm for all the series (see Table I and Fig. 3). The HA crystallite size seems to be less affected by the presence of the flux material.

One can also associate the increase of the grain size to the firing process that the film was submitted. The crystallite size of the HA is around 46 nm in the films of this series.

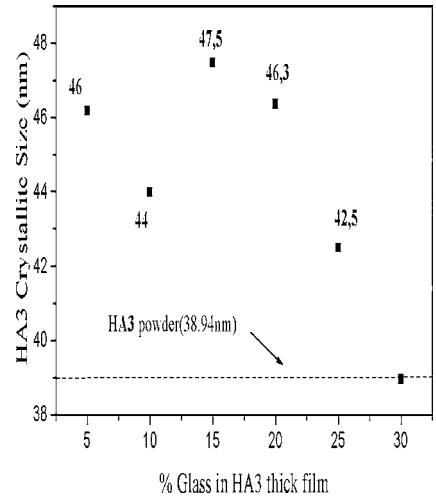

Figure 3 Crystallite size of the HA in the ceramic HA3 and thick films HA3G5, HA3G10, HA3G15, HA3G20 and HA3G25 (data from Fig. 1).

3.2. Scanning electron microscopy

The grain morphology of the films was investigated by means of SEM. In Figs 4–7 one has the samples HA3G5, HA3G10, HA3G20 and HA3G25 with a 5000X amplification factor. Comparing Figs 4–7 one can notice that the scanning electron photomicrograph of the films revealed that the presence of the glass is leading to a spherical morphology for the synthesized particles in film HA3G5 (Fig. 4). With the increase of the presence of the glass the grains are aggregating together forming plates for sample HA3G10 and HA3G20 (see Figs 5 and 6). However this a quite dynamic process. For sample HA3G25 (see Fig. 7) the spherical morphology for the grains is dominant again. The kind of grain clustering behavior will be very critical in the electrical properties of the films. Energy-dispersive spectroscopy (EDS) analysis (Fig. 8) showed that the main elements of the HA3 powder were carbon, oxygen, phosphorus and calcium. For the films HA3G5, HA3G10 and HA3G15 one has the same elements. The EDS of a crystal, present in the ceramic HA3 showed a mass ratio of Ca/P around 2.1 (see Table I). The theoretical expected value for HA is around Ca/P = 2.15. For the film with higher glass content (HA3G10 and HA3G15) it was observed a Ca/P ratio around 2.3 (see Table I). For the HA3G5 film the Ca/P ratio is around 1.62 which is below the expected value of 2.15. The presence of others phases in the HA film was detected in the X-ray analysis. For the HA3G15 (see Table I and Fig. 8, the mass ratio expected is around Ca/P = 2.15 and one actually has Ca/P = 2.37, which is good agreement with the expected value.

3.3. Dielectric measurements

In Fig. 1 one has the sample geometry we used for the dielectric measurements. Rectangular coordinates are assigned to the samples as shown in Fig. 1. The 2-1 plane is the sample plane, and the 3 axis is perpendicular to the plane of the sample. The thickness and the diameter of each sample are found in Table I.

In Fig. 9 one has the dielectric constant (K) measurements of the films (see Table I). One can notice that,

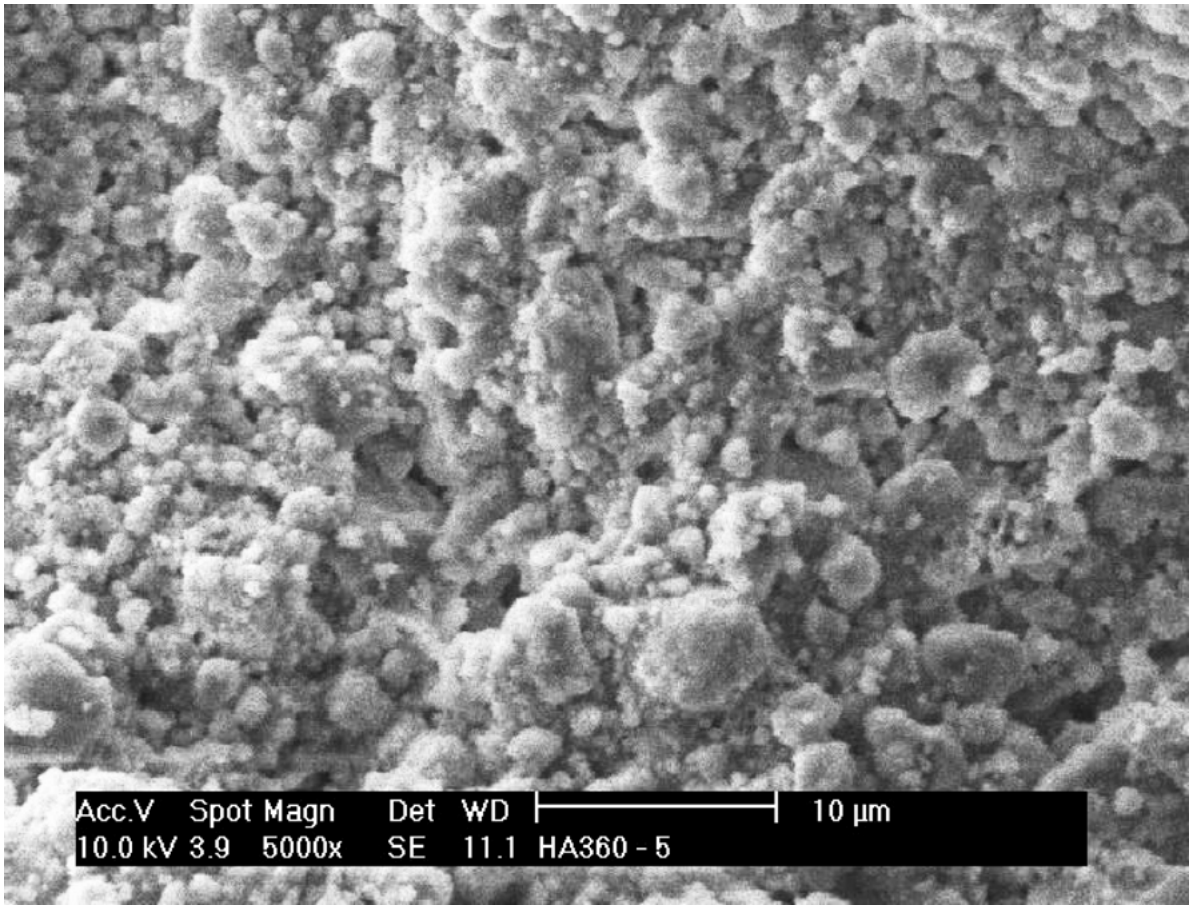

Figure 4 Scanning electron photomicrograph of the HA3G5 thick film (5000×).

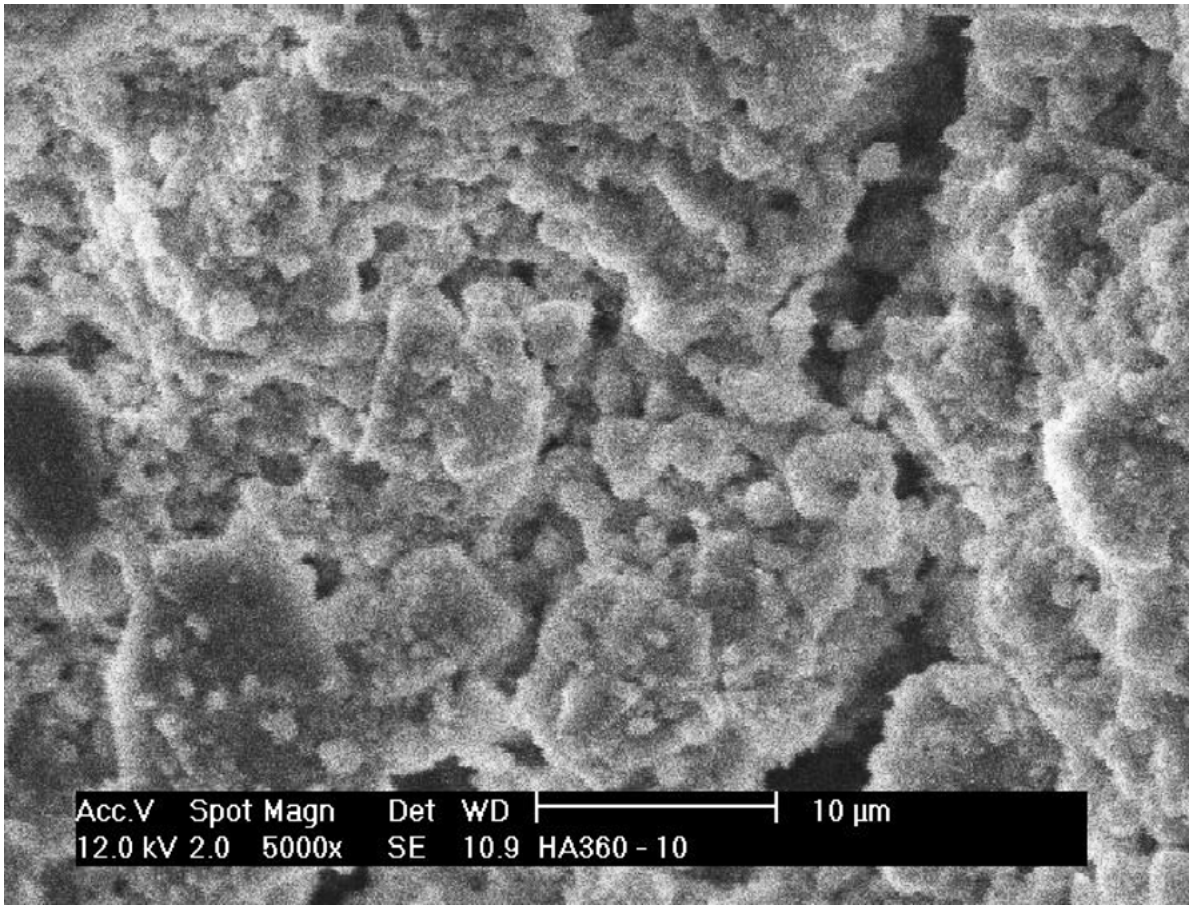

Figure 5 Scanning electron photomicrograph of the HA3G10 thick film (5000×).

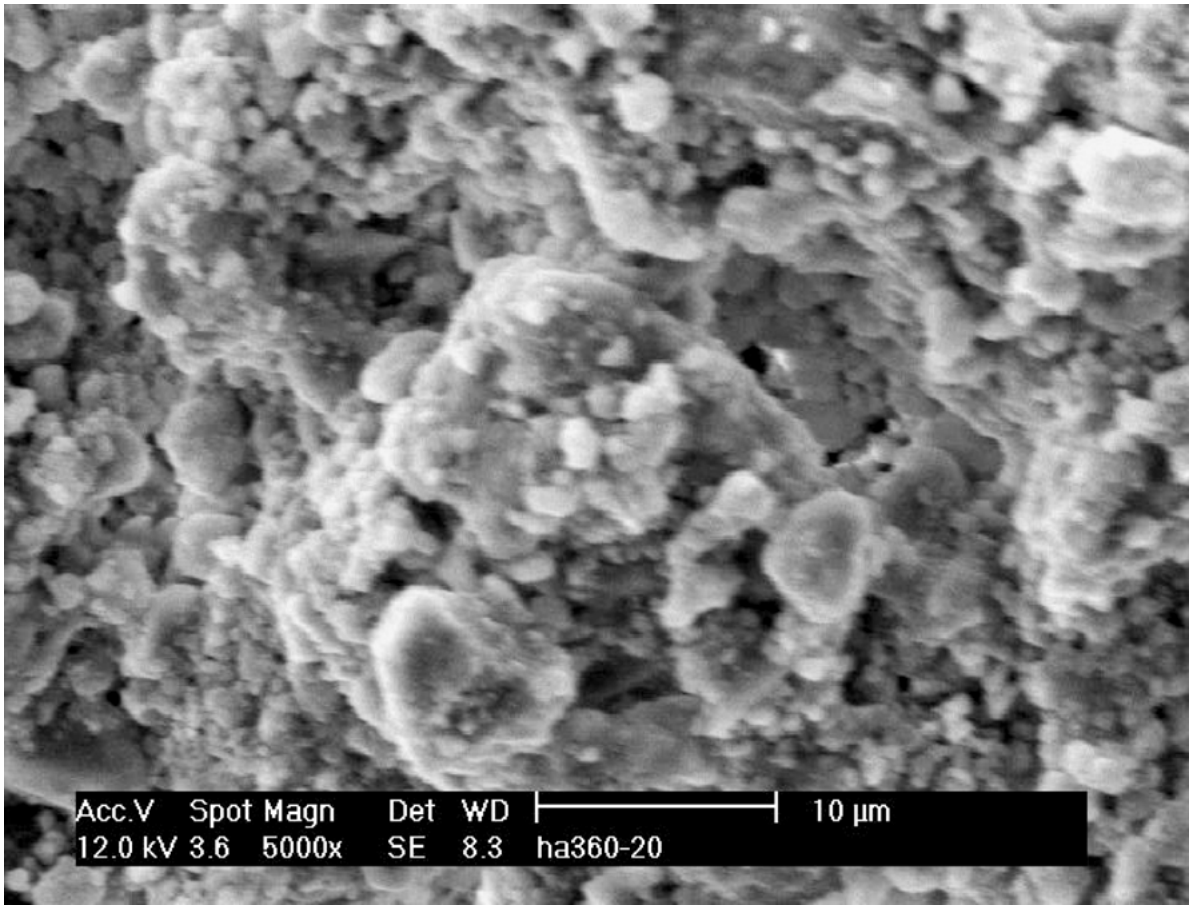

Figure 6 Scanning electron photomicrograph of the HA3G20 thick film (5000×).

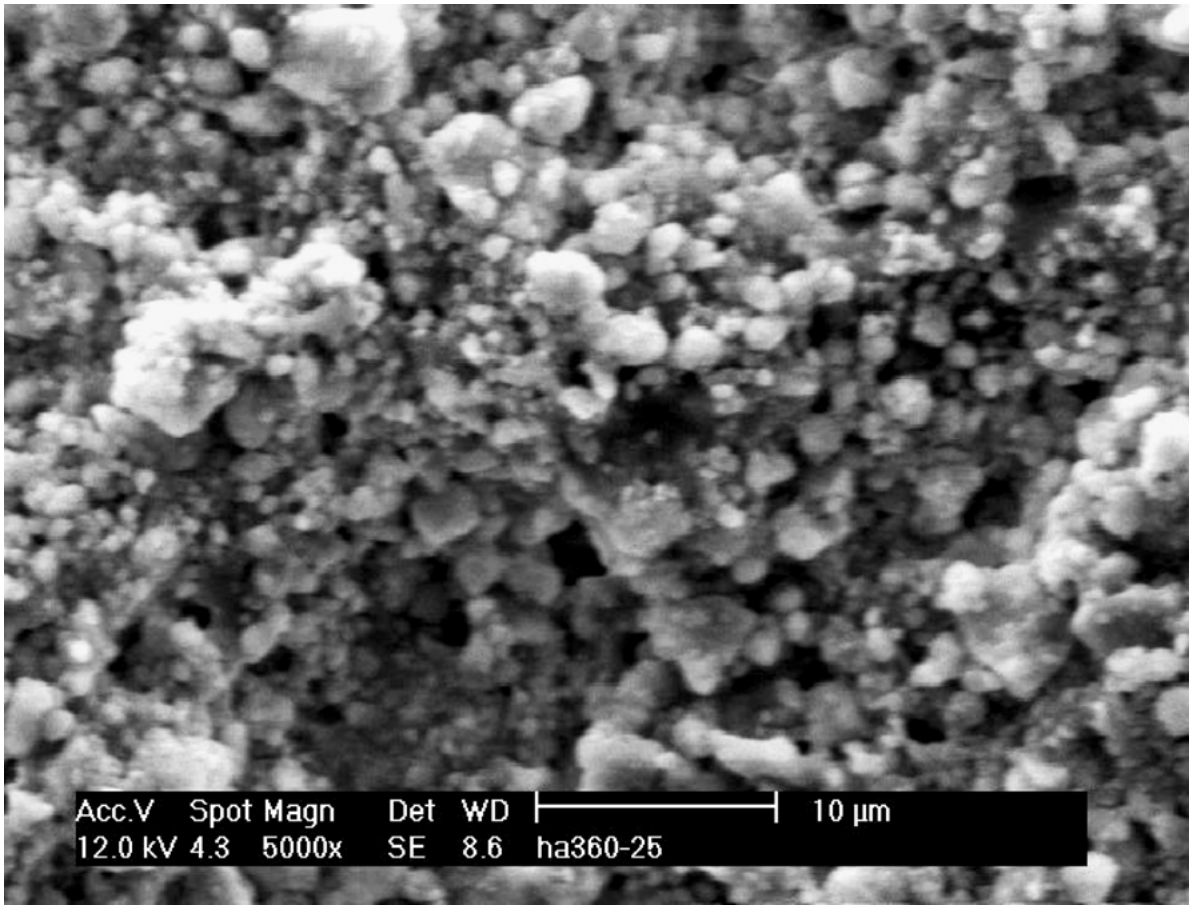

Figure 7 Scanning electron photomicrograph of the HA3G25 thick film (5000×).

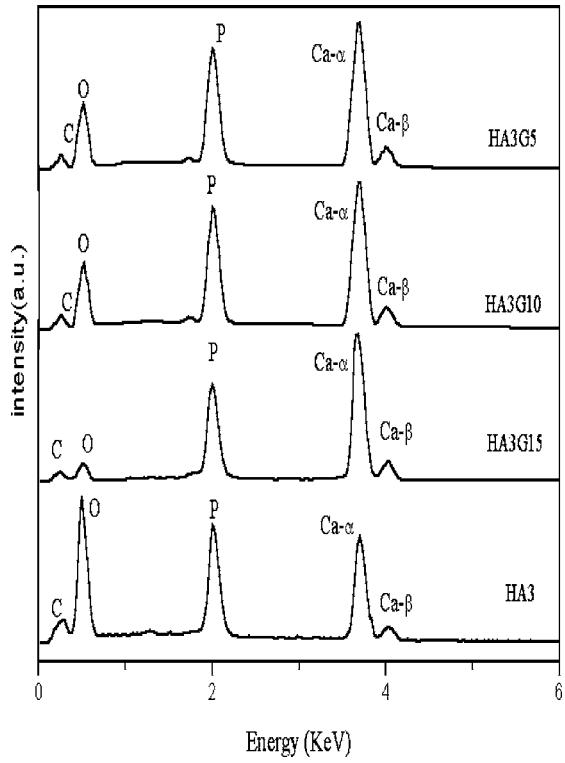

Figure 8 Energy Dispersive Spectroscopy of the ceramic HA3 and thick films HA3G5, HA3G10, HA3G15.

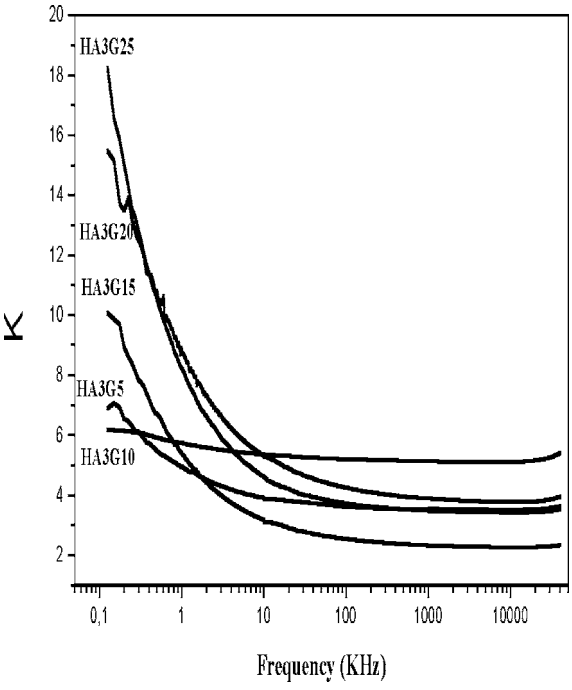

Figure 9 Dielectric permittivity (K) as a function of frequency of the HA3GY series.

for all the films there is a decrease of the DC with the increase of the frequency. The DC was studied in the frequency range of 100 Hz to 40 MHz. At low frequency (1 KHz) the DC is lower for HA3G5 film (see Table I), $K = 4.9$ and increase slightly with the increase of the glass concentration. For the film HA3G20 one has $K = 8.7$. This is an interesting behavior that could be associated to the micro structural behavior of the film that was observed in the SEM analysis. In the presence

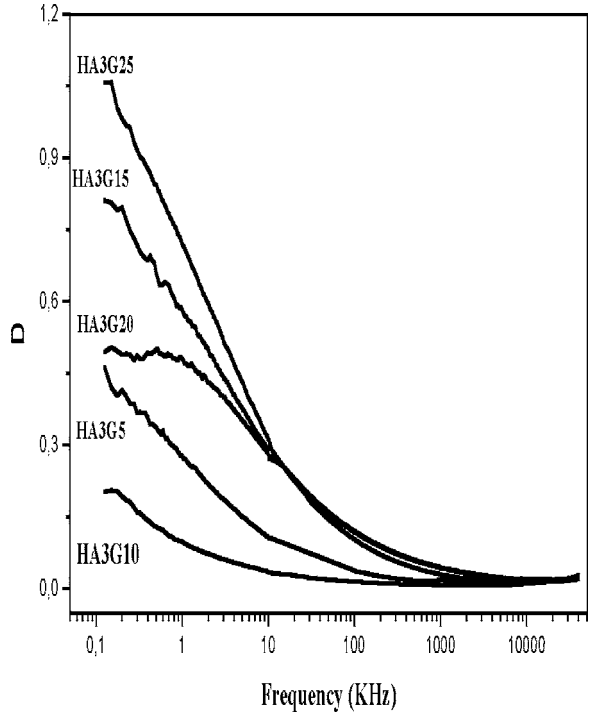

Figure 10 Dielectrc loss (D) as a function of frequency of the HA3GY series.

of the glass, a spherical morphology for the synthesized particles in film HA3G5 was observed (Fig. 4). With the increase of the presence of the glass the grains are aggregating together forming plates for sample HA3G10 and HA3G20. This microstructural process seems to be very critical in the electrical properties of the films.

These values of the dielectric constant are quite compatible with the values reported in the literature for thin films prepared by pulsed laser deposition [24] and sol-gel procedures [25]. For films prepared by pulsed laser deposition, present dielectric constant of 5.8 at 1 KHz [24].

In Fig. 10 one has loss tangent of the films. The loss is decreasing as we increase the frequency for all the films. The higher loss was observed for the high concentration of glass (HA3G25) with $D = 0.7$ at 1 KHz. The lower loss was obtained for HA3G10 ($D = 0.1$). For higher frequencies (1 MHz) the loss is lower, and for all films it is around (see Fig. 10) 10^{-2}. These values of DC and loss are similar to those of Al_2O_3 which is used conventionally for microwave applications [26].

4. Conclusions

In this paper we did a study on the structural and electrical properties of bioceramic hydroxyapatite (HA) thick films. The films were prepared in two layers using the screen printing technique on Al_2O_3 substrates. Mechanical alloying has been used successfully to produce nanocrystalline powders of hydroxyapatite (HA) to be used in the films. We also look for the effect of the grain size of the HA in the final properties of the film. The samples were studied using X-ray diffraction, scanning electron microscopy (SEM), electric and loss measurements. We did a study of the dielectric permittivity and the loss of the films in the radio-frequency of the spectra.

The X-ray diffraction (XRD) patterns of the films indicates that all the peaks associated to HA phase are present in the films. Extra peaks that are probably associated to the presence of the flux material (powder glass) were observed. One can also notice an increase of the crystallite size to the firing process that the film was submitted. The crystallite size of the HA in the films are around 46 nm .The particle morphology of the films was investigated by means of SEM. The presence of the glass is leading to a spherical morphology for the synthesized particles in the film. With the increase of the presence of the glass the grains are aggregating together forming plates. The kind of grain clustering behavior will be very critical in the electrical properties of the films. Energy-dispersive spectroscopy (EDS) analysis showed that the main elements of the HA film were carbon, oxygen, phosphorus and calcium. For the film with higher glass content it was observed, from the EDS analysis, that the Ca/P ratio around 2.3. The theoretical expected value for HA is around Ca/P = 2.15 which is good agreement with the expected value. One can notice that, for all the films there is a decrease of the DC with the increase of the frequency. The values of the dielectric constant of the films are in between 4 and 9 (at 1 KHz), as a function of the flux concentration. The loss is decreasing as we increase the frequency for all the films. The higher loss was observed for the high concentration of the flux material, with $D = 0.7$ at 1 KHz. The lower loss was obtained for low flux concentration ($D = 0.1$). For higher frequencies (1 MHz) the loss is lower, and for all films it is around 10^{-2}. These values of DC and loss are similar to those of Al_2O_3 which is used conventionally for microwave applications. This strongly suggests that the screen-printing HA thick films are good candidates for applications in biocompatible coatings of implant materials but also for the insulating materials of electronic circuits and dielectric layer in bio-sensors.

Acknowledgements

This work was partly sponsored by FINEP, CNPq, FUNCAP and CAPES (Brazilian agencies).

References

1. C. LAVERNIA and J. M. SCHOENUNG, *Bull. Amer. Ceram. Soc. Ceram. Bull.* **70** (1991) 95.
2. V. SERGO, O. SBAIZERO and D. R. CLARKE, *Biomaterials* **18** (1997) 477.
3. B. R. CONSTANTZ, I. C. ISON, M. T. FULMER *et al.*, *Science* **267** (1995) 1796.
4. M. J. YASZEMSK *et al.*, *Biomaterials* **17** (1996) 175.
5. H. S LIU *et al.*, *Ceramics International* **23** (1997) 19.
6. G. FELICIO FERNANDES *et al.*, *Quimica Nova* **23** (2000) 441.
7. G. HEIMKE, *Angew. Chem.* **101** (1989) 111.
8. L. L. HENCH, *J. Amer. Ceram. Soc.* **74** (1991) 1487.
9. M. R. BET *et al.*, *Quimica Nova* **20** (1997) 475.
10. P. DUCHEYNE *et al.*, *Biomaterials* **11** (1990) 244.
11. M. WEI *et al.*, *J. Biomed. Mater. Res.* **45** (1999) 11.
12. S. BAN *et al.*, *Jpn. J. Appl. Phys. Part 2, Lett.* **32**(10B) (1993) 1577.
13. C. M. COTELL, *Appl. Surf. Sci.* **69** (1993) 140.
14. L. TORRISI *et al.*, *Appl. Phys. Lett.* **62** (1993) 237.
15. L. D. PIVETEAU *et al.*, *J. Mater. Sci. Mater. Med.* **10** (1999) 161.
16. T. BRENDEL *et al.*, *ibid.* **3** (1992) 175.
17. E. RUCKENSTEIN *et al.*, *J. Colloid Interface Sci.* **63** (1983) 245.
18. C. M. COTELL *et al.*, *J. Appl. Biomat.* **3** (1992) 87.
19. R. K. SINGH *et al.*, *Biomaterials* **15** (1993) 522.
20. R. S. DE FIGUEIREDO, A. MESSAI, A. C. HERNANDES and A. S. B. SOMBRA, *J. Mater. Sci. Lett.* **17** (1998) 449.
21. I. F. VASCONCELOS *et al.*, *ibid.* **18** (1999) 1871.
22. I. F. VASCONCELOS, *ibid.* **36** (2001) 587.
23. M. N. TARAVEL, *Biomaterials* **16**(11) (1995) 865.
24. S. HONTSU *et al.*, *Thin Solid Films* **295** (1997) 214.
25. D. M. LIU *et al.*, *Biomaterials* **23** (2002) 691.
26. A. J. MOULSON and J. M. HERBERT, "Electroceramics" (Chapman and Hall, 1990).

Received 29 January
and accepted 7 July 2003